HNPS Advances in Nuclear Physics

Vol 30 (2024)

HNPS2023

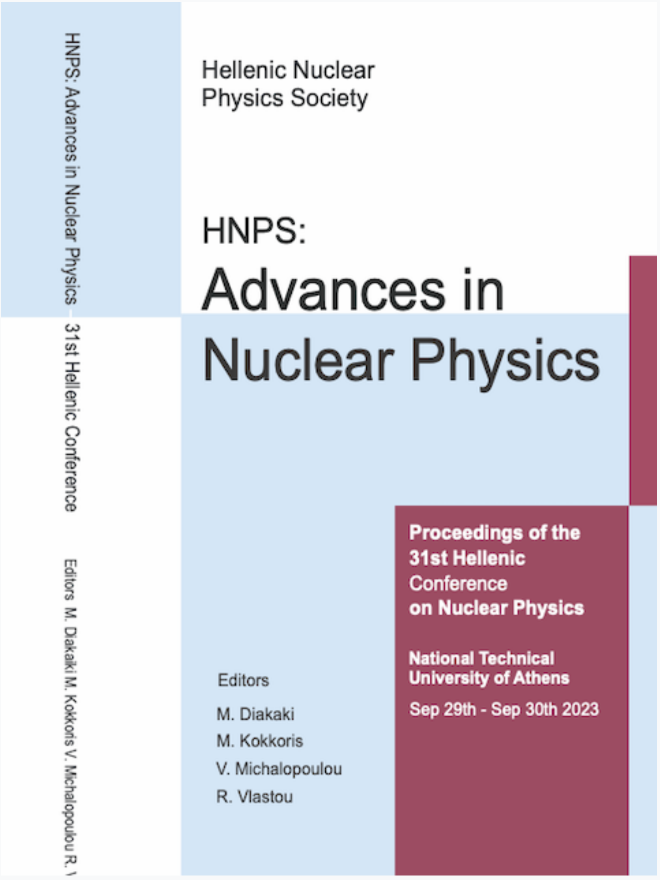

Shape/phase transitions and shape coexistence in even-even nuclei

Dennis Bonatsos, Andriana Martinou, Spyridon Peroulis, Theodoros Mertzimekis, Nikolay Minkov

doi: 10.12681/hnpsanp.6086

To cite this article:

Bonatsos, D., Martinou, A., Peroulis, S., Mertzimekis, T., & Minkov, N. (2024). Shape/phase transitions and shape coexistence in even-even nuclei. *HNPS Advances in Nuclear Physics*, *30*, 59–66. https://doi.org/10.12681/hnpsanp.6086

Shape/phase transitions and shape coexistence in even-even nuclei

D. Bonatsos[1,*], A. Martinou[1], S.K. Peroulis[1], T.J. Mertzimekis[2], N. Minkov[3]

[1] *Institute of Nuclear and Particle Physics, National Centre for Scientific Research "Demokritos", Aghia Paraskevi, GR-15310 Attiki, Greece*

[2] *Department of Physics, National and Kapodistrian University of Athens, Zografou Campus, GR-15784, Athens, Greece*

[3] *Institute of Nuclear Research and Nuclear Energy, Bulgarian Academy of Sciences, 72 Tzarigrad Road, 1784 Sofia, Bulgaria*

Abstract Shape/phase transitions have been observed in certain regions of the nuclear chart. Shape coexistence is also known to occur in various regions of the nuclear chart, forming islands. The interrelation between these two concepts is considered in the regions around (N=90, Z=60), (N=60, Z=40), (N=40, Z=34), in which shape coexistence due to proton-induced neutron particle-hole excitations is related to a first-order shape/phase transition from spherical to deformed shapes.

Keywords shape/phase transition, shape coexistence

A shape/phase transition (SPT) [1] corresponds to an abrupt change of the nuclear shape. In the parameter space of the Interacting Boson Model [2], a first-order SPT appears between spherical and axially symmetric deformed shapes, ending up at a point representing a second order SPT from spherical to γ-unstable (soft to triaxial deformation) shapes [3]. In the Bohr collective model framework [4], these SPTs have been described in terms of the critical point symmetries (CPS) X(5) [5] and E(5) [6], respectively. These CPS models provide parameter-independent (up to overall scales) predictions for the spectra and B(E2) transition rates at the critical point.The best experimental manifestations of the X(5) CPS have been found in the N=90 isotones ^{150}Nd, ^{152}Sm, and ^{154}Gd [7].

Shape coexistence (SC) [8,9] is said to occur when the ground state band (gsb) is accompanied by another K=0 band with similar energy but very different structure. For example, one of the bands can be spherical and the other one deformed, or both bands can be deformed, one of them having a prolate shape and the other an oblate shape.

Shape coexistence has been observed in several regions of the nuclear chart, but not all over it, as it was initially expected [8]. Martinou et al. in 2021 suggested [10,11] a dual shell mechanism in the framework of the proxy-SU(3) symmetry [12-14], which is an approximation to the nuclear shell model [15,16], predicting that SC can occur only within certain stripes on the nuclear chart, depicted in Fig. 1. These predictions were in good agreement with the schematic drawings of regions in which SC has been observed experimentally, reported in the review article by Heyde and Wood in 2011 [8], as seen in Fig. 2. They are also in agreement to the more recent collection of nuclei in which SC is expected to be seen, shown in Fig. 3, based on the review article by Bonatsos et al. in 2023 [9].

In the present article, we first try to impose some quantitative limits for the appearance of SC [17]. In Table 1, data are exhibited for all nuclei beyond Z=N=18 for which a K=0 band, as well as the transition rate $B(E2;0_2^+\to 2_1^+)$ are known [18]. The ratios $R_{0/2}=E(0_2^+)/E(2_1^+)$ and $B_{02}=B(E2;0_2^+\to 2_1^+)/B(E2;2_1^+\to 0_1^+)$ are also shown, along with the ratio $R_{4/2}=E(4_1^+)/E(2_1^+)$, a well known indicator of collectivity.

* Corresponding author: *bonat@inp.demokritos.gr*

In Fig. 4(a) the data for the ratio B_{02} are plotted vs. the data for the ratio $R_{0/2}$. A clear separation is seen into two parts, a region of high B_{02} values appearing at low $R_{0/2}$ values on the left, and a region of low B_{02} values appearing at high $R_{0/2}$ values on the right, separated by the *N*=90 isotones corresponding to the X(5) CPS mentioned above. The same behavior is seen in the predictions of various theoretical models, plotted in Fig. 4(b). From Table 1 and Fig. 4 one concludes that SC can appear when the conditions $R_{0/2} < 5.7$ and $B_{02} > 0.1$ are simultaneously fulfilled.

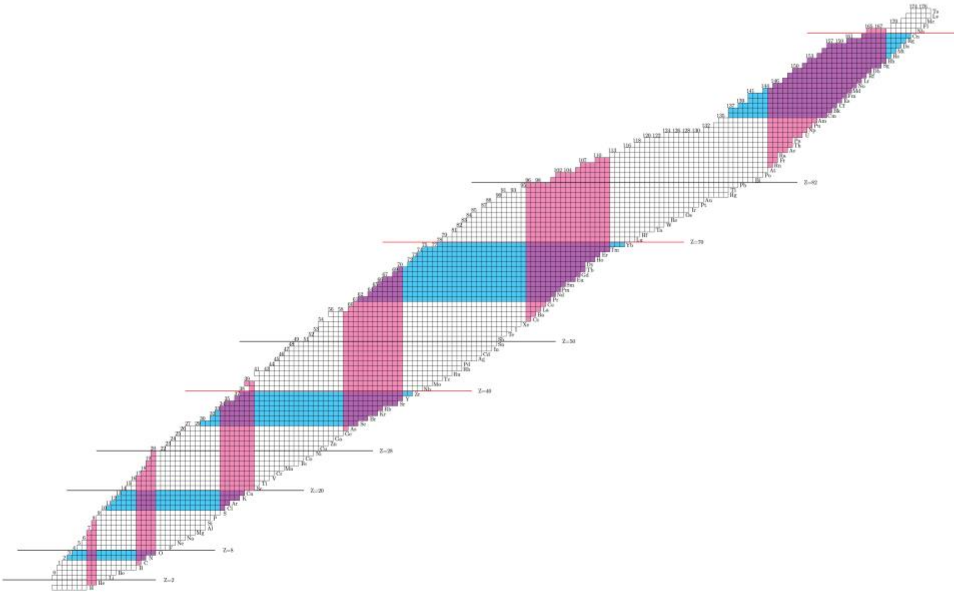

Figure 1. *Stripes in which SC can occur according to the dual shell mechanism[10,11] of the proxy-SU(3) symmetry [12-14]. Adapted from Ref. [10].*

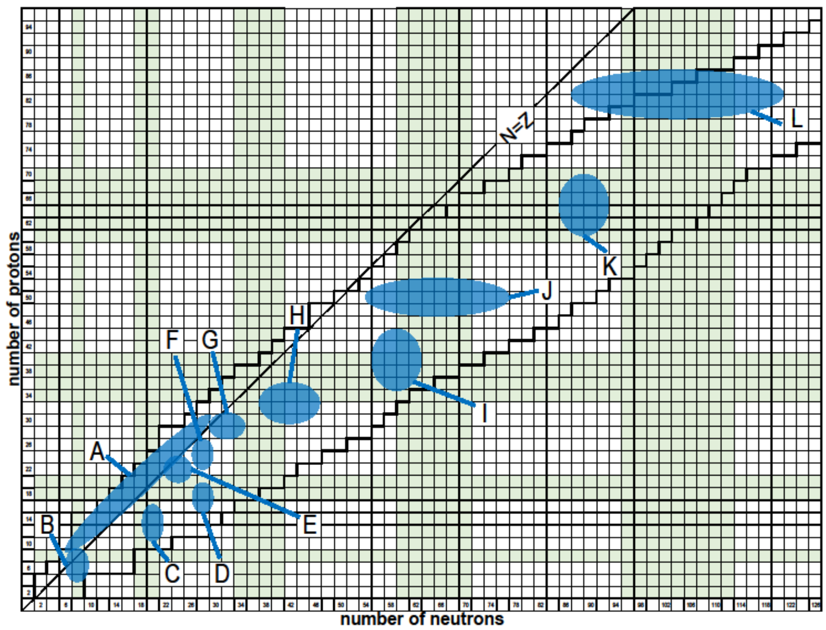

Figure 2. *Regions in which SC has been observed, as given in the review article [8], are depicted in blue and are compared to the green stripes in which SC is allowed to occur, according to the dual shell mechanism [10,11] within the proxy-SU(3) model [12-14]. Adapted from Ref. [9].*

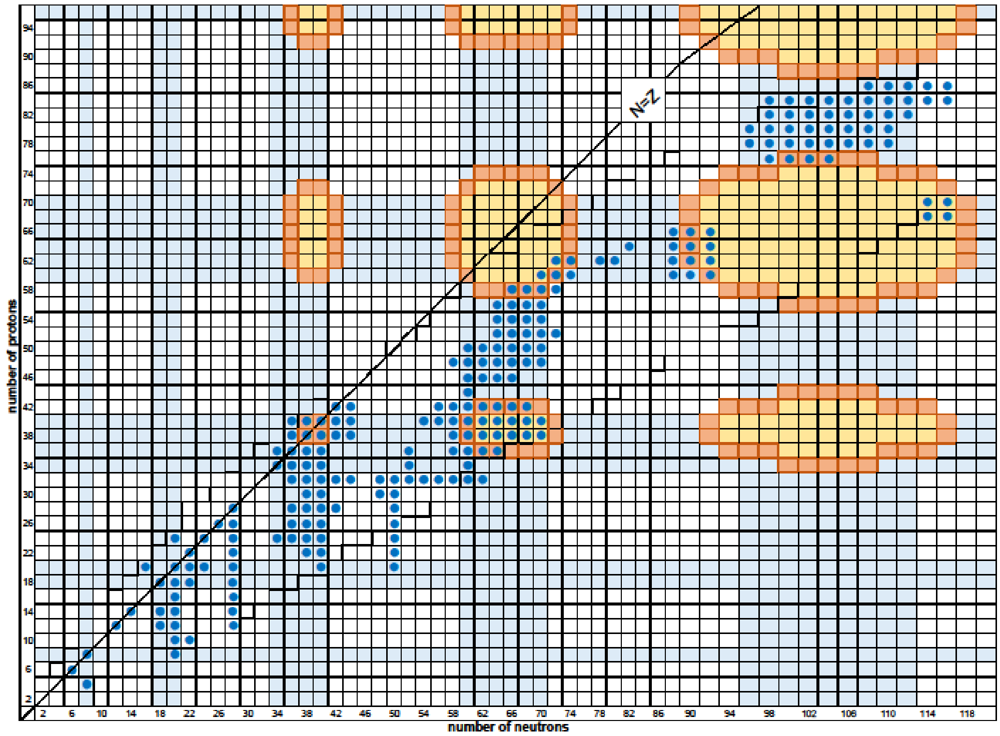

Figure 3. *Nuclei exhibiting SC according to the review article [9] are shown, together with azure stripes in which SC is allowed to occur according to the dual shell mechanism [10,11] within the proxy-SU(3) model [12-14], and the orange contours corresponding to P=5 [21], showing the borders of the regions of well deformed nuclei, depicted in yellow. Adapted from Ref. [9].*

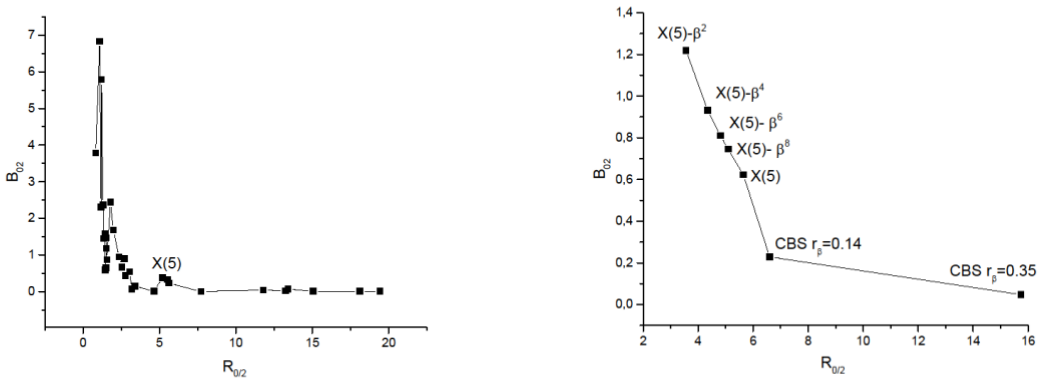

(a)

(b)

Figure 4. *(a) Experimental B_{02} ratios plotted vs. $R_{0/2}$ ratios. (b) The same plot for predictions by the theoretical models X(5) [5], X(5)-β^{2n} (n=2,4,6,8) [19], CBS [20]. Adapted from Ref. [17].*

In Fig. 5 nuclei from Table 1 with ratios $R_{4/2}=E(4_1^+)/E(2_1^+)$ below 3.05 are shown by green triangles, while nuclei with R4/2 above 3.05 are depicted by blue triangles. SC is expected for nuclei fulfilling the condition $R_{4/2}<3.05$, which lie outside the orange contours, which correspond to values of the P-factor $P=N_pN_n/(N_p+N_n)$ [21] close to 5, where N_p (N_n) is the number of valence protons (neutrons) in a given nucleus, counted from the closest closed shell. Deformed nuclei with $R_{4/2}>3.05$ lie in the yellow regions inside the orange contours and are not expected to exhibit SC. What is interesting, is that the N=90 isotones being the best experimental manifestations of the X(5) CPS fall on or near the orange contours, indicating that SC is indeed seen in these critical nuclei.

Table 1. *Nuclei beyond Z=N=18 with experimentally known [18] K=0 bands (with energy levels given in keV) and B(E2; $0_2^+ \rightarrow 2_1^+$) transition rates (given in W.u.). Adapted from Ref. [17]. See text for further discussion.*

nucleus	$R_{4/2}$	$E(2_1^+)$	$E(0_2^+)$	$B(E2;2_1^+\rightarrow 0_1^+)$	$B(E2; 0_2^+\rightarrow 2_1^+)$	$R_{0/2}$	B_{02}
^{40}Ar	1.980	1460.8	2120.9	9.0 (4)	5.3 (8)	1.452	0.589
^{40}Ca		5629.4	3352.6	0.143 (+35-24)	7.5 (+30-20)	0.639	52.558
^{42}Ca	1.805	1524.7	1837.3	9.5 (4)	55. (5)	1.205	5.789
^{70}Ge	2.071	1039.5	1215.6	20.8 (4)	48. (7)	1.169	2.308
^{72}Ge	2.072	834.0	691.4	23.5 (4)	89.0 (15)	0.829	3.787
^{72}Se	1.899	862.1	937.2	23.7 (17)	162. (28)	1.087	6.835
^{96}Sr	2.000	814.9	1229.3	13. (8)	15.3 (16)	1.509	1.177
^{98}Sr	3.006	144.2	215.6	96. (3)	62. (+7-6)	1.495	0.646
^{98}Zr	1.674	1222.9	854.0	2.9 (+8-5)	145. (+40-30)	0.698	50.000
^{100}Zr	2.656	212.5	331.1	77. (2)	67. (6)	1.558	0.870
^{100}Mo	2.121	535.6	695.1	37.6 (9)	89. (3)	1.298	2.367
^{102}Mo	2.507	296.6	698.3	74. (9)	70. (30)	2.354	0.946
^{104}Ru	2.482	358.0	988.3	57.9 (11)	25. (3)	2.761	0.432
^{110}Pd	2.463	373.8	946.7	55.5 (9)	37. (4)	2.533	0.667
^{112}Cd	2.292	617.5	1224.3	30.31 (19)	51. (14)	1.983	1.683
^{116}Cd	2.375	513.5	1380.3	33.5 (12)	30. (6)	2.688	0.896
^{114}Sn	1.683	1299.9	1953.3	15. (3)	22. (8)	1.503	1.467
^{116}Sn	1.848	1293.6	1756.9	12.4 (4)	18. (3)	1.358	1.452
^{118}Sn	1.854	1229.7	1758.3	12.1 (15)	19. (3)	1.430	1.570
^{126}Xe	2.424	388.6	1313.9	44. (4)	6.4 (12)	3.381	0.145
^{148}Nd	2.493	301.7	916.9	57.9 (22)	3.12 (22)	3.039	0.539
^{150}Nd	2.927	130.2	675.9	116. (3)	43.1 (23)	5.191	0.372
^{152}Sm	3.009	121.8	684.8	145.0 (16)	33.3 (12)	5.622	0.230
^{154}Sm	3.255	82.0	1099.3	176. (1)	12. (3)	13.406	0.068
^{152}Gd	2.194	344.3	615.4	73. (+7-6)	178. (+33-53)	1.787	2.438
^{154}Gd	3.015	123.1	680.7	157. (1)	52. (8)	5.530	0.331
^{156}Gd	3.239	89.0	1049.5	189. (3)	8. (+4-7)	11.792	0.042
^{158}Gd	3.288	79.5	1196.2	198. (5)	1.17 (+418-13)	15.047	0.006
^{166}Er	3.289	80.6	1460.0	217. (5)	2.7 (10)	18.114	0.012
^{172}Yb	3.305	78.7	1042.9	212. (2)	3.6 (10)	13.252	0.017
^{174}Yb	3.310	76.5	1487.1	201. (7)	1.4 (+11-5)	19.439	0.007
^{186}Os	3.165	137.2	1061.0	93.6 (21)	0.066	7.733	0.001
^{192}Os	2.820	205.8	956.5	62.1 (7)	0.57 (12)	4.648	0.009
^{196}Pt	2.465	355.7	1135.3	40.60 (20)	2.8 (15)	3.192	0.069
X(5)	2.904					5.649	0.624

In corroboration of the above findings, data are exhibited in Table 2 for all nuclei beyond *Z*=*N*=18 for which a K=0 band, as well as the transition rate B(E2; $0_2^+\rightarrow 2_1^+$) are known [18], but no levels beyond 0_2^+ are known for the K=0 band [18]. Nuclei from Table 2 with ratios $R_{4/2}=E(4_1^+)/E(2_1^+)$ below 3.05 are added in Fig. 5 as green circles, while nuclei with R4/2 above 3.05 are depicted by blue circles.

It should be noticed that from Fig. 5 are absent the neutron-deficient Hg, Pb, and Po isotopes, which form the first region in which SC [8,9] has been observed, the reason being that no data for their B(E2; $0_2^+\rightarrow 2_1^+$) rates are shown in Ref. [18]. Existing data for these nuclei have been collected in Table 3, while these nuclei are shown as purple diamonds in Fig. 5 for completeness.

Table 2. *Nuclei beyond Z=N=18 with experimentally known $B(E2; 0_2^+ \rightarrow 2_1^+)$ transition rates (given in W.u.) [18], but with no other levels of a K=0 band based on the 0_2^+ known. Energy levels are given in keV. Adapted from Ref. [17]. See text for further discussion.*

nucleus	$R_{4/2}$	$E(2_1^+)$	$E(0_2^+)$	$B(E2;2_1^+\rightarrow 0_1^+)$	$B(E2; 0_2^+\rightarrow 2_1^+)$	$R_{0/2}$	B_{02}
^{38}Ar		2167.5	3376.9	3.40 (16)	1.26 (8)	1.558	0.371
^{44}Ca	1.973	1157.0	1883.5	10.9 (6)	22. (7)	1.628	2.018
^{48}Ca	1.175	3831.7	4283.3	1.84 (+17-14)	10.1 (5)	1.118	5.489
^{46}Ti	2.260	889.3	2611.0	19.5 (6)	50. (14)	2.936	2.564
^{48}Ti	2.344	983.5	2997.2	13.2 (+13-11)	20.6 (+44-32)	3.047	1.561
^{50}Ti	1.722	1553.8	3868.3	5.46 (19)	1.6 (+14-5)	2.490	0.293
^{54}Cr	2.185	834.9	2829.6	14.4 (6)	10. (+3-4)	3.389	0.694
^{56}Fe	2.462	846.8	2941.5	16.8 (7)	2.4 (+7-12)	3.474	0.143
^{58}Ni	1.691	1454.2	2942.6	10.0 (4)	0.00040 (6)	2.023	$4\ 10^{-5}$
^{64}Ni	1.940	1345.8	2867.3	7.76 (26)	3.15 (+23-21)	2.131	0.406
^{64}Zn	2.326	991.6	1910.3	20.0 (5)	0.057 (3)	1.927	0.003
^{68}Zn	2.244	1077.4	1655.9	14.69 (19)	5.5 (10)	1.537	0.374
^{70}Zn	2.019	884.9	1070.8	16.7 (10)	37.3 (19)	1.210	2.234
^{74}Ge	2.457	595.9	1482.8	33.0 (4)	9. (+9-6)	2.489	0.273
^{74}Se	2.148	634.7	853.8	42.0 (6)	77. (7)	1.345	1.833
^{76}Se	2.380	559.1	1122.3	44. (1)	47. (22)	2.007	1.068
^{78}Se	2.449	613.7	1498.6	33.5 (8)	1.17 (21)	2.442	0.035
^{80}Se	2.554	663.3	1478.8	24.7 (6)	6.9 (11)	2.220	0.279
^{82}Se	2.650	654.8	1410.3	17.3 (10)	3.62	2.154	0.209
^{74}Kr	2.225	455.6	509.0	67. (1)	60. (17)	1.117	0.896
^{78}Kr	2.460	455.0	1017.2	67.9 (22)	47. (4)	2.235	0.692
^{82}Kr	2.344	776.5	1487.6	21.3 (9)	15. (5)	1.916	0.704
^{88}Sr		1836.1	3156.2	7.6 (4)	4.0 (+15-14)	1.719	0.526
^{90}Zr	1.407	2186.3	1760.7	5.38 (13)	26. (50)	0.805	4.833
^{92}Zr	1.600	934.5	1382.8	6.4 (6)	14.4 (5)	1.480	2.250
^{94}Zr	1.600	918.8	1300.2	4.9 (3)	9.4 (4)	1.415	1.918
^{96}Mo	2.092	778.2	1148.1	20.7 (4)	51. (7)	1.475	2.464
^{98}Mo	1.918	787.4	734.8	20.1 (4)	48.5 (+50-125)	0.933	2.413
^{96}Ru	1.823	832.6	2148.8	18.4 (4)	12 (+5-12)	2.581	0.652
^{98}Ru	2.142	652.4	1322.1	29.8 (10)	42. (+12-11)	2.026	1.409
^{100}Ru	2.273	539.5	1130.3	35.7 (3)	35. (5)	2.095	0.980
^{102}Ru	2.329	475.1	943.7	44.6 (7)	35. (6)	1.986	0.785
^{104}Pd	2.381	551.8	1333.6	36.9 (19)	13.2 (13)	2.417	0.358
^{106}Pd	2.402	511.9	1133.8	44.3 (15)	35. (8)	2.215	0.790
^{108}Pd	2.416	433.9	1052.8	50.4 (15)	52. (5)	2.426	1.032
^{114}Cd	2.299	558.5	1285.6	31.1 (19)	27.4 (17)	2.032	0.881
^{118}Cd	2.388	487.8	1134.5	33. (3)	5.3 (8)	2.636	0.161
^{120}Sn	1.873	1171.3	1875.1	11.41 (22)	12.6 (17)	1.601	1.104
^{124}Te	2.072	602.7	1657.3	31.1 (5)	20. (4)	2.750	0.643
^{126}Te	2.043	666.4	1873.4	25.1 (5)	8.8 (+8-11)	2.811	0.351
^{144}Nd	1.887	696.6	2084.7	25.9 (5)	19. (12)	2.993	0.734
^{150}Sm	2.316	334.0	740.5	57.1 (13)	53. (5)	2.217	0.928
^{194}Pt	2.470	328.5	1267.2	49.5 (20)	0.63 (+20-13)	3.858	0.013
^{198}Pt	2.419	407.2	914.5	31.81 (22)	26. (7)	2.246	0.817

doi: 10.12681/hnpsanp.6086

Table 3. *Hg, Pb, and Po isotopes known to exhibit SC, for which the 0_2^+ state is experimentally known [18]. Energies are given in keV, while transition rates are given in W.u. Adapted from Ref. [17]. See text for further discussion.*

nucleus	$R_{4/2}$	$E(2_1^+)$	$E(0_2^+)$	$B(E2;2_1^+\rightarrow 0_1^+)$	$R_{0/2}$
^{180}Hg	1.623	434.2	419.8	49. (9)	0.967
^{182}Hg	3.198	351.7	328.0	55. (3)	0.933
^{184}Hg	2.962	366.8	375.1	62. (15)	1.023
^{186}Hg	2.665	405.3	523.0	71.3 (13)	1.290
^{188}Hg	2.434	412.8	824.5	54. (9)	1.997
^{190}Hg	2.502	416.3	1278.6	45. (3)	3.071
^{184}Pb			570.0		
^{186}Pb			530.0		
^{188}Pb	1.470	723.6	591.0	7. (3)	0.817
^{190}Pb	1.588	773.9	658.0		0.850
^{192}Pb	1.588	853.6	768.8		0.901
^{194}Pb	1.596	965.1	930.7		0.964
^{196}Po	1.924	463.1	558.0		1.205
^{198}Po	1.915	604.9	816.0		1.349
^{200}Po	1.918	665.9	1136.5		1.707

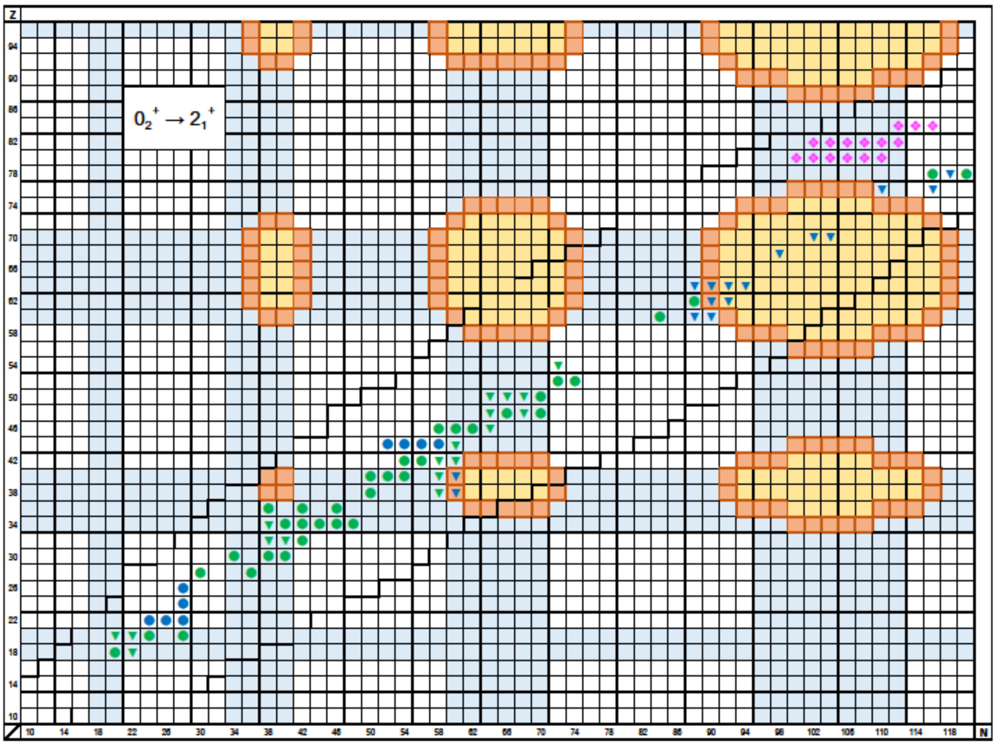

Figure 5. *Nuclei with $R_{4/2}$<3.05 in which SC is expected are shown by green symbols, while nuclei with $R_{4/2}$>3.05, for which no SC is expected, are indicated by blue symbols.Hg, Pg, and Po isotopes known to exhibit SC are shown by purple diamonds. Adapted from Ref. [17]. See text for further discussion.*

In Fig. 5, nuclei in regions lighter than N=90 also fall on or near the orange contours. In order to examine if they do exhibit critical behavior, we need a relevant order parameter. It turns out [17,22] that the ratio $R_{2/0}=1/R_{0/2}$ is an appropriate order parameter. Indeed, using the standard IBM Hamiltonian in the consistent-Q formalism [23] with the parameter ζ playing the role of the control parameter (with ζ=0 corresponding to spherical shapes and ζ=1 corresponding to deformed cases), we see in Fig. 6(a) that the ratio $R_{2/0}$ uncovers the critical point of the transition from spherical to deformed shapes, in the same way the ratio $R_{4/2}$ does, as seen in Fig. 6(b).

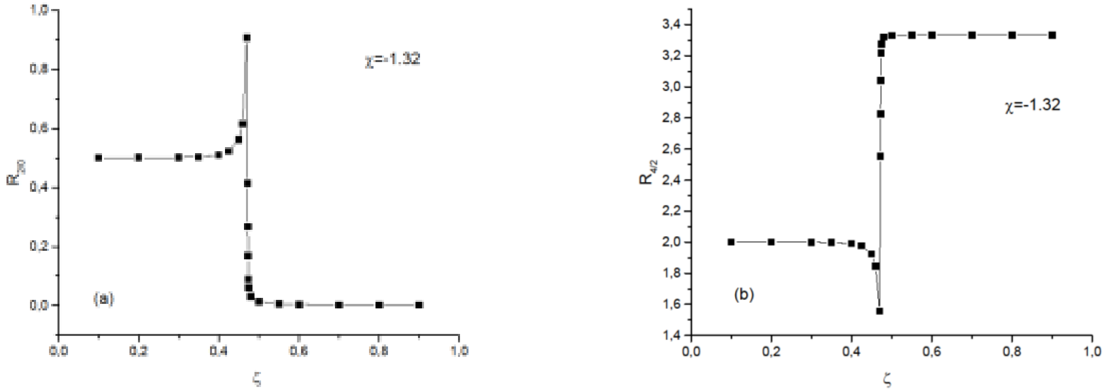

(a) *(b)*

Figure 6. *Energy ratios $R_{2/0}$ (a) and $R_{4/2}$ (b) plotted vs. the control parameter ζ, as obtained from IBM calculations using the consistent-Q formalism Hamiltonian [23]. Adapted from Ref. [17].*

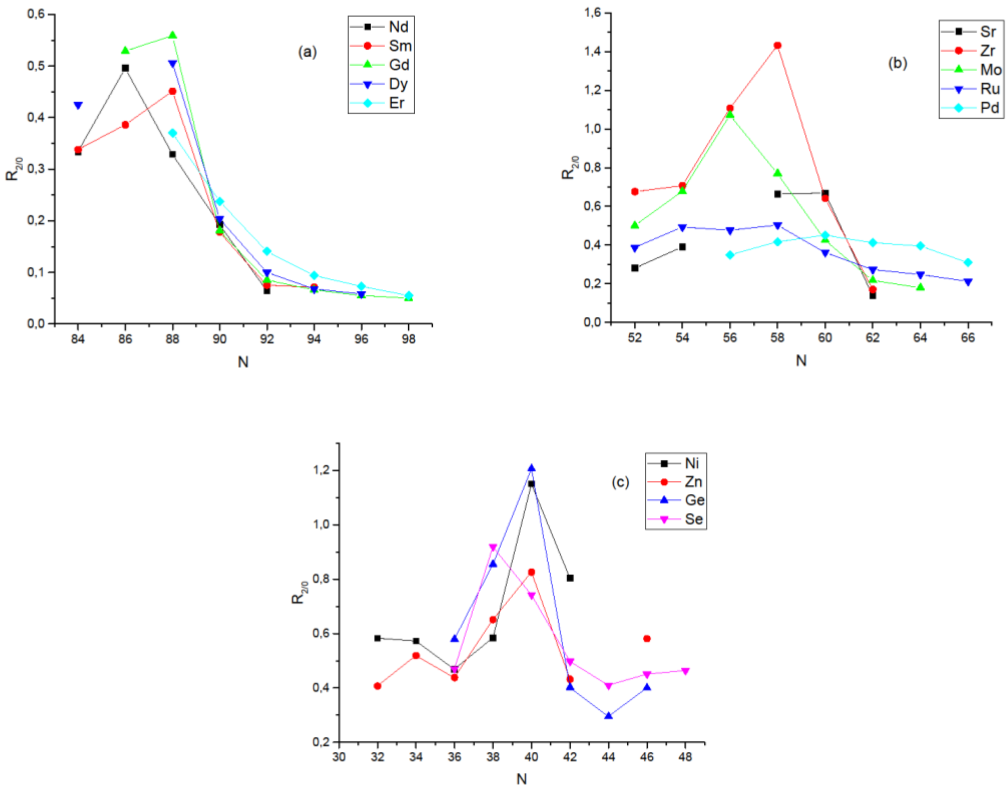

Figure 7. *Experimental energy ratios $R_{2/0}$ in the Nd-Er (a), Sr-Pd (b), and Ni-Se (c) regions, plotted vs. the neutron number N, which serves as the control parameter. Adapted from Ref. [17].*

In Fig. 7 the data for the ratio $R_{2/0}$ are shown in three different regions, with the neutron number *N* serving as the control parameter. The critical behavior seen in Fig. 7(a) for the *N*=90 isotones in the Nd-Er region, is also observed in Fig. 7(b) for the *N*=60 isotones in the Sr-Pd region, as well as in Fig. 7(c) for the N=40 isotones in the Ni-Se region, in which SC due to proton-induced particle-hole excitations is known to occur [24,25].

In conclusion, a close connection between SPT and SC is proved to exist in the three regions (N=90,Z=60), (N=60,Z=40), and (N=40,Z=34). The close connection between SPTs and SC in the last two regions has been studied in detail by Heyde [26] and Garcia-Ramos [27,28].

Acknowledgments

Support by the Bulgarian National Science Fund (BNSF) under Contract No. KP-06-N48/1 is gratefully acknowledged.

References

[1] P. Cejnar et al., Rev. Mod. Phys. 82, 2155 (2010); doi: 10.1103/RevModPhys.82.2155
[2] F. Iachello and A. Arima, The Interacting Boson Model (Cambridge U. Press, Cambridge, 1987); doi: 10.1017/CBO9780511895517
[3] D.H. Feng et al., Phys. Rev. C 23, 1254 (1981); doi: 10.1103/PhysRevC.23.1254
[4] A. Bohr, Dan. Mat. Fys. Medd. 26, no. 14 (1952)
[5] F. Iachello, Phys. Rev. Lett. 87, 052502 (2001); doi: 10.1103/PhysRevLett.87.052502
[6] F. Iachello, Phys. Rev. Lett. 85, 3580 (2000); doi: 10.1103/PhysRevLett.85.3580
[7] R.F. Casten and E. A. McCutchan, J. Phys. G 34, R285 (2007); doi: 10.1088/0954-3899/34/7/R01
[8] K. Heyde and J.L. Wood, Rev. Mod. Phys. 83, 1467 (2011); doi: 10.1103/RevModPhys.83.1467
[9] D. Bonatsos et al., Atoms 11,117 (2023); doi: 10.3390/atoms11090117
[10] A. Martinou et al., Eur. Phys. J. A 57, 84 (2021); doi: 10.1140/epja/s10050-021-00396-w
[11] A. Martinou et al., Symmetry 15, 29 (2023); doi: 10.3390/sym15010029
[12] D. Bonatsos et al., Phys. Rev. C 95, 064325 (2017); doi: 10.1103/PhysRevC.95.064325
[13] D. Bonatsos et al., Phys. Rev. C 95, 064326 (2017); doi: 10.1103/PhysRevC.95.064326
[14] D. Bonatsos et al., Symmetry 15, 169 (2023); doi: 10.3390/sym15010169
[15] A. Martinou et al., Eur. Phys. J. A 56, 239 (2020); doi: 10.1140/epja/s10050-020-00239-0
[16] D. Bonatsos et al., Eur. Phys. J. Plus 135, 710 (2020); doi: 10.1140/epjp/s13360-020-00749-2
[17] D. Bonatsos et al., J. Phys. G 50, 075105 (2023); doi: 10.1088/1361-6471/acd70b
[18] ENSDF database; url: https://www.nndc.bnl.gov/ensdf
[19] D. Bonatsos et al., Phys. Rev. C 69, 014302 (2004); doi: 10.1103/PhysRevC.69.014302
[20] N. Pietralla and O.M. Gorbachenko, Phys. Rev. C 70, 011304(R) (2004); doi:10.1103/PhysRevC.70.011304
[21] R.F. Casten et al., Phys. Rev. Lett. 58, 658 (1987); doi: 10.1103/PhysRevLett.58.658
[22] D. Bonatsos et al., Phys. Rev. Lett. 100, 142501 (2008); doi: 10.1103/PhysRevLett.100.142501
[23] D.D. Warner and R.F. Casten, Phys. Rev. Lett. 48, 1385 (1985); doi: 10.1103/PhysRevLett.48.1385
[24] D. Bonatsos et al., Phys. Lett. B 829, 137099 (2022); doi: 10.1016/j.physletb.2022.137099
[25] D. Bonatsos et al., Phys. Rev. C 106, 044323 (2022); doi: 10.1103/PhysRevC.106.044323
[26] K. Heyde et al., Phys. Rev. C 69, 054304 (2004); doi: 10.1103/PhysRevC.69.054304
[27] J.-E. Garcia-Ramos and K. Heyde, EPJ Web of Conf. 178, 05005 (2018); doi: 10.1051/epjconf/201817805005
[28] J.-E. Garcia-Ramos and K. Heyde, Phys. Rev. C 102, 054333 (2020); doi: 10.1103/PhysRevC.102.054333